Temperature Drives Epidemics in a Zooplankton-Fungus Disease System: A Trait-Driven Approach Points to Transmission via Host Foraging

Marta S. Shocket,[1,*] Alexander T. Strauss,[1,†] Jessica L. Hite,[1,‡] Maja Šljivar,[1] David J. Civitello,[1,§] Meghan A. Duffy,[2] Carla E. Cáceres,[3] and Spencer R. Hall[1]

1. Department of Biology, Indiana University, Bloomington, Indiana 47405; 2. Department of Ecology and Evolutionary Biology, University of Michigan, Ann Arbor, Michigan 48109; 3. School of Integrative Biology, University of Illinois at Urbana-Champaign, Urbana, Illinois 61801

Submitted January 30, 2017; Accepted October 10, 2017; Electronically published February 5, 2018

Online enhancements: appendix. *Dryad data:* http://dx.doi.org/10.5061/dryad.3k8m3.

ABSTRACT: Climatic warming will likely have idiosyncratic impacts on infectious diseases, causing some to increase while others decrease or shift geographically. A mechanistic framework could better predict these different temperature-disease outcomes. However, such a framework remains challenging to develop, due to the nonlinear and (sometimes) opposing thermal responses of different host and parasite traits and due to the difficulty of validating model predictions with observations and experiments. We address these challenges in a zooplankton-fungus (*Daphnia dentifera–Metschnikowia bicuspidata*) system. We test the hypothesis that warmer temperatures promote disease spread and produce larger epidemics. In lakes, epidemics that start earlier and warmer in autumn grow much larger. In a mesocosm experiment, warmer temperatures produced larger epidemics. A mechanistic model parameterized with trait assays revealed that this pattern arose primarily from the temperature dependence of transmission rate (β), governed by the increasing foraging (and, hence, parasite exposure) rate of hosts (f). In the trait assays, parasite production seemed sufficiently responsive to shape epidemics as well; however, this trait proved too thermally insensitive in the mesocosm experiment and lake survey to matter much. Thus, in warmer environments, increased foraging of hosts raised transmission rate, yielding bigger epidemics through a potentially general, exposure-based mechanism for ectotherms. This mechanistic approach highlights how a trait-based framework will enhance predictive insight into responses of infectious disease to a warmer world.

Keywords: temperature, infectious disease, fungal disease, transmission rate, *Daphnia*, *Metschnikowia*.

* Corresponding author. Present address: Department of Biology, Stanford University, Stanford, California 94305; e-mail: mshocket@stanford.edu.

† Present address: Department of Ecology, Evolution, and Behavior, University of Minnesota, St. Paul, Minnesota 55108.

‡ Present address: School of Biological Sciences, University of Nebraska, Lincoln, Nebraska 68588.

§ Present address: Department of Biology, Emory University, Atlanta, Georgia 30322.

ORCIDs: Strauss, http://orcid.org/0000-0003-0633-8443; Civitello, http://orcid.org/0000-0001-8394-6288.

Am. Nat. 2018. Vol. 191, pp. 435–451.
DOI: 10.1086/696096

Introduction

How will climate change impact infectious diseases? This question is difficult to answer, often controversial, and yet crucial to resolve in our warming world. About 15 years ago, concern arose that a warmer world would generate widespread increases in infectious disease (e.g., Harvell et al. 2002). However, in the current prevailing view, climate change will have important but idiosyncratic impacts on infectious disease: some diseases will increase, some will decrease, and others will simply shift their geographic range (Lafferty 2009; Altizer et al. 2013). Thus, it is critical to develop theory for thermal disease ecology that accounts for different temperature-disease relationships within a general predictive framework (Rohr et al. 2011; Altizer et al. 2013). This framework must be hypothesis driven, field tested, and founded on mechanisms and functional traits that drive the temperature dependence of disease (Rohr et al. 2011; Altizer et al. 2013; Rodó et al. 2013). Furthermore, it should apply across a broad variety of transmission modes, hosts, parasites, and habitats (Altizer et al. 2013).

Several challenges have hindered this mechanistic framework for the thermal effects on disease spread. First, temperature affects multiple components of the transmission process simultaneously (Rohr et al. 2011). The thermal responses of different host or parasite traits often have opposing effects on disease spread, making the net outcome unclear. In the classic example, the maturation time of malaria parasites

and mosquito life span both decrease with temperature; the former increases transmission, while the latter decreases it, because for transmission to occur, a mosquito must survive long enough for the parasites to reach maturity (Rogers and Randolph 2006; Paaijmans et al. 2009). Therefore, meaningful predictions require resolving tension between many traits via quantification of the whole transmission process. Second, these conflicting traits typically have nonlinear responses to temperature (Angilletta 2006; Rohr et al. 2011; Mordecai et al. 2013). Thus, characterizing their reaction norms requires fitting nonlinear functions to data that cover the relevant temperature gradient with sufficient resolution. Third, it can be difficult to validate predictions from mechanistic models with field observations. Long-term data sets of outbreaks in nature are costly to assemble and scarce. Fourth, the trait-based, whole-transmission approach has largely focused on mosquito-borne diseases of humans. This important but narrow scope currently limits a theory for the thermal ecology of disease: breadth is needed with other types of hosts and transmission modes. Additionally, while human diseases have important health consequences, field observations are influenced by social factors and interventions, and experimental manipulations can be unethical (Altizer et al. 2013). Thus, comparing model predictions with field data and demonstrating mechanistic causality is even more difficult for human diseases. These four challenges have limited our ability to create a predictive, mechanistic framework for temperature-based regulation of disease spread.

In this study, we use a freshwater zooplankton-fungus disease system to overcome these four challenges. First, we build a model of disease spread that captures the transmission ecology in terms of host and parasite traits. Second, we parameterize these traits with nonlinear functions across the relevant temperature gradient via experiments with the easily cultured host and parasite. Third, we compare the model predictions for epidemic size to patterns from a field survey of epidemics in lakes. In the field survey, epidemics vary greatly in size and starting temperature, providing substantial variation to explain. We also test causality using mesocosm experiments that manipulate temperature. Finally, the system's natural history shares features with many other systems but is not well represented in current thermal disease theory (but see Hall et al. 2006). Because hosts eat spores produced by an obligate killer fungus, the thermal response of foraging (exposure) rate and spore production from dead hosts could be critical. Thus, we are able to rigorously broaden a predictive, mechanistic framework for the temperature dependence of infectious disease.

Our analysis uses a combination of field surveys, parameterized mathematical models, and a mesocosm experiment to test the hypothesis that warmer temperatures promote disease. A six-year survey of fungal epidemics in *Daphnia* host populations demonstrates that epidemics that start during warmer temperatures (i.e., earlier in the season) grow larger ("Field Survey"). We establish mechanistic links between temperature and epidemic size with a mathematical model based on the study system's natural history ("Temperature-Dependent Model") and parameterized using several experimental assays ("Parameterizing Temperature-Dependent Traits") or literature values. With these temperature-dependent functions, we calculated a synthetic index of disease spread, R_0. This approach resolves tension between the conflicting thermal responses of two key traits: transmission rate and parasite production ("Predicting Disease Spread: R_0"). The analysis found that increasing transmission rate dominates, so warmer temperatures should indeed cause larger epidemics. We tested this prediction using a mesocosm experiment. The experiment echoed the field pattern: epidemics grew exponentially larger in warmer conditions ("Tests of Predictions: Mesocosm Experiment"), while parasite production remained fairly flat (therefore, less important). This result echoed similar results in the field ("Spore Load in Natural Epidemics"), prompting our conclusion that higher transmission rate leads to larger epidemics in warmer conditions.

Methods and Results

Study System

The focal hosts (*Daphnia dentifera*; hereafter, hosts) are dominant zooplankton grazers in many freshwater, temperate lakes across the Midwestern United States (Tessier and Woodruff 2002). Some populations experience epidemics of the virulent fungal parasite *Metschnikowia bicuspidata* (hereafter, fungus; Hall et al. 2010*b*; Penczykowski et al. 2014*a*). Hosts become infected when they filter feed nonselectively on phytoplankton and inadvertently consume fungal spores (Hall et al. 2007). The fungal spores pierce through the host's gut wall, entering the host body cavity. Once inside, the fungus replicates, producing spores and eventually killing the host. Following host death, fungal spores are released into the water column where new hosts can consume them (Ebert 2005). Many traits that influence the spread of the parasite (e.g., demographic traits of hosts, probability of infection, and production of spores) change plastically with temperature (Hall et al. 2006). Epidemics typically begin in late summer or early fall (August–October) and wane in late fall or early winter (November–December; Hall et al. 2011; Penczykowski et al. 2014*a*). Maximum prevalence can reach up to 60% (Penczykowski et al. 2014*a*). During this time period, weighted temperature of lake water (defined below in "Field Survey") declines from ~25°C to ~5°C. Thus, epidemics that begin earlier experience warmer temperatures than those starting later.

Field Survey

Methods. We tested whether warmer conditions were associated with larger epidemics using 6 years of field data. We surveyed 10–28 lakes per year in southwestern Indiana (Greene and Sullivan counties) on a weekly (2009–2011) or biweekly (2013–2015) basis from August to December, yielding data for 74 epidemics. For each visit, we collected a zooplankton sample (by pooling three vertical tows of a 13-cm-diameter Wisconsin net with 153 μm mesh) and measured lake water temperature data at 0.5- to 1-m intervals with a Hydrolab multiprobe (Hach Environmental, Loveland, CO). We visually diagnosed at least 400 live hosts from the zooplankton sample with a dissecting scope (×20–×50 magnification).

From these field data, we took two temperature and two disease metrics. The temperature metrics account for variation in realized thermal environments of hosts. The effective temperature depends on daily vertical migration between upper, warmer waters (epilimnion, during night) and deeper, colder waters (hypolimnion, during day) of these often stratified (dimictic) lakes. The proportion of hosts that migrate below the epilimnion during the day varies between lakes (S. R. Hall, unpublished data). Thus, two measures of temperature bracket two extremes of migration. First, a mean epilimnetic temperature assumes no vertical migration. Second, a time-weighted temperature based on day length assumes that all hosts migrate down to the colder, deeper layer during the day (hereafter, weighted temperature; see appendix, available online, for details; Hall et al. 2005). In reality, most lakes likely fall somewhere between these two extremes. Then, we calculated two disease metrics. An epidemic started on the date when infection prevalence first exceeded 1% and was maintained above 1% for at least two consecutive sampling visits. (This choice eliminated false starts.) Epidemic size was calculated by integrating the area under the prevalence time series using the trapezoid rule (Penczykowski et al. 2014*a*; Strauss et al. 2015).

We fit linear mixed effects models predicting epidemic size as a function of lake, year, and temperature at the start of epidemics using the nlme package (Pinheiro and Bates 2000; Pinheiro et al. 2009) in R (R Core Team 2016). We performed model selection according to Bolker et al. (2009) and Zuur et al. (2009). Lake and year were included as random effects. We log transformed epidemic size to meet the assumption of normally distributed residuals. This transformation resulted in an exponential (rather than linear) relationship between temperature and epidemic size. We calculated the marginal R^2 value (variance explained by fixed effects, i.e., temperature at epidemic start) using the MuMIn package (Bartoń 2009; Nakagawa and Schielzeth 2013). We tested the significance of fixed and random factors using likelihood ratio tests. The data and code for all analyses in this article are deposited in the Dryad Digital Repository: http://doi.org/10.5061/dryad.3k8m3 (Shocket et al. 2018).

Results. Fungal epidemics that start earlier and warmer grow larger (fig. 1). More specifically, the field data show an exponential relationship between epidemic size and both measures of lake water temperature at the start of epidemics (fig. 1*A*, 1*B*; $P < .0001$ compared to null model [without temperature] for both measures of temperature; weighted temperature slope coefficient = 0.228 [95% confidence interval (CI): 0.175–0.281], epilimnetic temperature slope coefficient = 0.173 [95% CI: 0.140–0.206]). In both models, temperature at the epidemic start explains 43% of the variation in epidemic size (marginal $R^2 = 0.430$ for weighted temperature and 0.434 for epilimnetic temperature). In both models, the random effect for lake was significant ($P = .0001$ for weighted temperature, and $P = .0004$ for epilimnetic temperature), but the random effect for year was not ($P = 1$ for weighted temperature, and $P = .14$ for epilimnetic temperature). This field pattern suggests that temperature could contribute to variation in epidemic size. However, temperature could be confounded with other biotic or abiotic factors also changing seasonally. Therefore, we turn to a mechanistic model and experiment to examine the causal relationship between temperature and epidemic size.

Temperature-Dependent Model

We used a temperature-explicit model of the zooplankton-fungus system to determine how the thermal responses of host and parasite traits govern disease spread. In this mathematical model, key traits of the host and parasite (i.e., model parameters) vary as functions of temperature. The model without temperature notation is

$$\frac{dS}{dt} = e f A(S + I) - dS - \beta SZ, \tag{1a}$$

$$\frac{dI}{dt} = \beta SZ - d_i I, \tag{1b}$$

$$\frac{dZ}{dt} = d_i I \, \sigma_{\max}\left(\frac{A}{A + h}\right) - mZ - f(S + I)Z, \tag{1c}$$

$$\frac{dA}{dt} = r_A A\left(1 - \frac{A}{K_A}\right) - f(S + I)A \tag{1d}$$

(see also table 1). Susceptible hosts (S; eq. [1a]) increase via births from susceptible and infected (I) classes; hosts feed at the same foraging rate (f) on algae (A) and produce offspring with conversion efficiency (e). (Infection does not reduce fecundity in this model.) Susceptible hosts decrease at background death rate d and become infected at transmission rate β after encountering fungal spores (Z). Infected hosts (eq. [1b]) are lost at disease-elevated death rate $d_i > d$. Dead infected hosts release spores (eq. [1c]) following a saturating func-

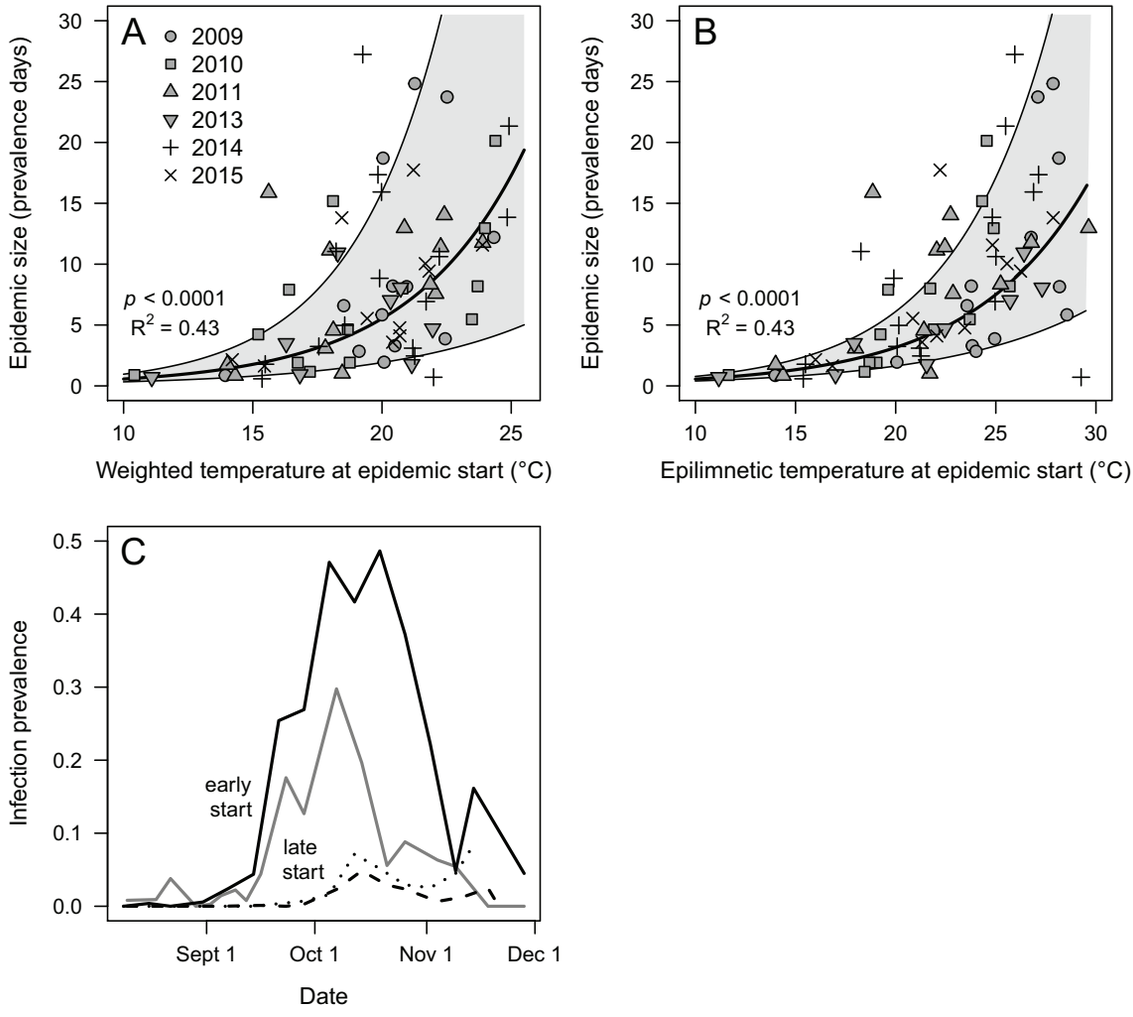

Figure 1: *A*, *B*, Field data from 6 years support temperature as a potential driver of disease: epidemic size (summed area under the curve of time series of infection prevalence) increases exponentially with weighted temperature (*A*) and epilimnetic temperature (*B*) of lake water at the start of the epidemic. Each point is a lake in a single year. The thick lines are linear mixed effects models fit to log-transformed epidemic size data, with lake and year as random effects ($P < .0001$ compared to null model [without temperature] and marginal $R^2 = 0.43$ for both measures of temperature; weighted temperature slope coefficient = 0.228 [95% confidence interval (CI): 0.175–0.281], epilimnetic temperature slope coefficient = 0.173 [95% CI: 0.140–0.206]). Gray shading shows 95% CIs for the temperature slope coefficients. *C*, Examples of epidemic time series from four lakes in 2010: two epidemics that start early in the year (solid black and gray lines) reach higher prevalence and are bigger compared to two epidemics that start later in the year (dotted and dashed lines).

tion of algal resource density with a maximal spore yield (σ_{max}) and a half-saturation constant (h; Hall et al. 2009*b*; Strauss et al. 2015). Spores are lost at a background rate (m) and by the foraging of susceptible and infected hosts, $f(S + I)$. Algal resources (eq. [1d]) grow logistically with a maximal per capita growth rate (r_A) and carrying capacity (K_A). They are eaten by susceptible and infected hosts.

We parameterized foraging rate (f), conversion efficiency (e), transmission rate (β), background and disease-elevated death rates (d and d_i), maximal spore yield (σ_{max}), algal-specific growth rate (r_A), and algal carrying capacity (K_A) as functions of temperature (see "Parameterizing Temperature-Dependent Traits"). Given lack of data, we assume that background spore loss (m) and spore production's half-saturation constant (h) do not vary with temperature.

Parameterizing Temperature-Dependent Traits

Methods: Experimental Assays. To parameterize the model, we measured traits over a temperature gradient that covers the most relevant part of the thermal range in which the hosts and epidemics occur (approximately 15°, 18°, 20°, 22°,

Table 1: Traits (parameters) for the mathematical model (eq. [1])

Parameter	Meaning (units)	Function type	Function coefficients (95% CIs) or values	Source
f	Host foraging rate (L/day)	Arrhenius function of T with power function of body length (L): $f(T,L) = L^{\gamma} \cdot f_R \cdot e^{T_A([1/T_R]-[1/T])}$	$\gamma = 2.15$ (1.71–2.63), $f_R = 5.39 \cdot 10^{-3}$ ($4.19–5.80 \cdot 10^{-3}$), $T_A = 8{,}740$ (6,220–11,600)	Foraging assay
β_{adult}	Transmission rate for adult hosts ($L = 1.5$ mm; $L \cdot \text{spore}^{-1} \cdot \text{day}^{-1}$)	Arrhenius function of T: $\beta_{\text{adult}}(T) = \beta_R \cdot e^{T_A([1/T_R]-[1/T])}$	$\beta_R = 1.05 \cdot 10^{-5}$ ($.893–1.23 \cdot 10^{-5}$), $T_A = 12{,}200$ (8,240–16,400)	Infection assay
u	Spore infectivity (spore^{-1})	Derived function of T: $u = \frac{\beta_{\text{adult}}}{f_{\text{adult}}}$	…	Foraging assay, infection assay
β_{pop}	Transmission rate for population ($L = .85$ mm; $L \cdot \text{spore}^{-1} \cdot \text{day}^{-1}$)	Derived function of T: $\beta_{\text{pop}} = u \cdot f_{\text{pop}}$	…	Foraging assay, infection assay
d	Uninfected host death rate (day^{-1})	Arrhenius function of T: $d(T) = d_R \cdot e^{T_A([1/T_R]-[1/T])}$	$d_R = .0118$ ($6.72 \cdot 10^{-3}$ – .0187), $T_A = 13{,}000$ (2,820–24,200)	Life table
d_i	Infected host death rate (day^{-1})	Arrhenius function of T: $d_i(T) = d_{iR} \cdot e^{T_A([1/T_R]-[1/T])}$	$d_{iR} = .0566$ (.0440–.0706), $T_A = 5{,}390$ (971–10,600)	Life table
r	Host per capita growth rate (day^{-1})	Arrhenius function of T: $r(T) = r_R \cdot e^{T_A([1/T_R]-[1/T])}$	$r_R = .325$ (.314–.335), $T_A = 3{,}900$ (3,210–4,610)	Life table
b	Host birthrate (day^{-1})	Derived function of T: $b = r + d$	…	Life table
e	Host conversion efficiency (births/μg Chl$a$)	Derived function of T: $e = b/(f \cdot A)$	…	Foraging assay, life table
$\sigma_{\max}$	Maximal spore yield (spores $\cdot 10^4$/host)	Quadratic function of T: $\sigma_{\max}(T) = \alpha_2 \cdot T^2 + \alpha_1 \cdot T + \alpha_0$	$\alpha_2 = -.149$ ($-.242$–$-.0550$), $\alpha_1 = 6.42$ (2.50–10.2), $\alpha_0 = -53.2$ (-92.0–-13.9)	Life table
r_A	Algal specific growth rate (day^{-1})	Arrhenius function of T (alternate format): $r_A(T) = c\, e^{(A-[E_a/R]\cdot[1/T])}$	$A = 19.7$ (day^{-1}), $E_a = 49.3$ (kJ mol^{-1}), R, gas constant ≈ 8.31 (J K^{-1} mol^{-1}), c (scaling) $= .27$	Modified from Xin et al. 2011
K_A	Algal carrying capacity (μg Chl$a$/L)	Linear function of T: $K_A(T) = c(\alpha_1 \cdot \text{T} + \alpha_0)$	$\alpha_1 = .101$, $\alpha_0 = -21.5$, c (scaling) $= 4$	Modified from Xin et al. 2011
H	Half-saturation constant of $\sigma(A)$ (μg Chl$a$)	Parameter does not vary with T	$h = 2.88$	Strauss et al. 2015
M	Background spore loss rate (spores/day)	Parameter does not vary with T	$m = .9$	

Note: Posterior distribution medians for coefficients (with 95% credible intervals [CIs]) are given for traits or parameters fit as functions of temperature. The spore yield function was fit with temperature in degrees Celsius. All other functions were fit with temperature in Kelvin. Parameters that vary with temperature are shown across a temperature gradient in figure 2. Coefficients: T_A = Arrhenius temperature; T_R = reference (R) temperature (20°C = 293.15 K). Parameters f_R, d_R, d_{iR}, and r_R denote reference value at T_R.

and 26°C, varying slightly among experiments; see fig. 2). Hosts cannot be cultured in constant temperatures above 27°C (M. S. Shocket, unpublished data), while infection develops extremely slowly at 10°C (Hall et al. 2006). Trait measurements came from a foraging assay, an infection assay, and a life table. Each of these is outlined briefly below; see appendix for details and parameter estimation. All experiments used a single clonal genotype of the host isolated from a lake in Michigan due to logistical constraints on the size of experiments. This clone is relatively susceptible to fungal infection (Hall et al. 2010*a*, 2012) and shows a representative thermal reaction norm for growth rate (fig. A1; figs. A1–A3 are available online).

Foraging assay. We collected foraging rate data across gradients of temperature and host body length (L). Foraging rate in *Daphnia* depends on both (Kooijman 2009), and our analysis requires foraging rate estimates for two different body sizes. The transmission assays used large adults ($L = 1.5$ mm), while mean body size in the mesocosm experiment and natural populations is much smaller ($L \approx 0.85$ mm, the size we used in simulations; M. S. Shocket, unpublished data). We selected individuals from each temperature treatment (16°, 18°, 21°, 24°, 27°C) that spanned a wide size gradient. Hosts were placed into individual tubes containing a known volume of algae suspended in filtered lake water and allowed to forage for 8.5 h. We used fluorometry to compare the amount of algae remaining in the grazed tubes to ungrazed controls.

Infection assay. We measured transmission rate (β) via the infection assay. For each temperature treatment, replicate beakers of six 5-day-old hosts (all reared at 20°C, average $L = 1.5$ mm) were exposed to a fixed dose (100 spores/mL) of spores for 24 h. Ten to 18 days later (depending on temperature), we diagnosed the infection status of the hosts and calculated the proportion of hosts infected in each beaker. We estimated the transmission rate for large adults (β_{adult}) from these data by fitting a temperature-dependent model. However, this calculation overestimates the transmission rate for mixed-age host populations, which are typically juvenile dominated (Hite et al. 2016). Because host foraging rate (f) is size dependent, large adults contact more spores and are more likely to become infected (Hall et al. 2007). We estimated a population-level transmission rate (β_{pop}) by adjusting for the lower foraging rate of smaller-bodied hosts found in a typical natural population ($L \approx 0.85$ mm). First, we divide the adult transmission rate by the adult foraging rate to calculate the per-spore infectivity (u): $u = \beta_{\text{adult}}/f_{\text{adult}}$. Then we multiply spore infectivity by the foraging rate for the population average body size so that $\beta_{\text{pop}} = u \cdot f_{\text{pop}}$. This breakdown allows analysis of each underlying mechanisms' contribution—host-parasite contact and spore infectivity—to the temperature dependence of transmission rate (β). The population-level transmission rate (hereafter, β) was used in all subsequent analyses of disease spread (i.e., R_0 calculation, sensitivity analysis, and epidemic simulations).

Life table. Most other traits were parameterized by a life table experiment. We estimated maximal spore yield ($\sigma_{\max}$), death rates of susceptible and infected hosts (d and d_i, respectively), and intrinsic rate of increase of hosts (r) directly from the life table. For each temperature treatment, we created two cohorts of same-age hosts; one was exposed to a high dose of parasite spores. We monitored individually housed hosts daily for survival and offspring production (yielding d and d_i from survival models and r estimated from the Euler-Lotka equation). We ground up dead infected hosts to count spores produced within each individual. Spore production at the high algal density used (2.0 mg dry/L) approximates maximal spore yield ($\sigma_{\max}$; Hall et al. 2009*b*; Strauss et al. 2015). We calculated conversion efficiency of host births (e) with data from the life table and the foraging assay. First, we calculated the host birthrate (b) as the sum of host intrinsic rate of increase (r) and background death rate (d): $b = r + d$. Then, we assumed birthrate equals assimilated energy converted into offspring, $e\,f\,A$ (eq. [1a]), where f is per capita foraging rate for large, adult hosts ($L = 1.5$ mm) on algae (A, converting 2.0 mg dry/L to 23.23 μg Chl*a*/L). Conversion efficiency was then estimated as $e = b/(f\,A)$.

Literature-based parameters. Parameter values for algal growth and the half-saturation constant (h) in the spore yield function came from the literature. We used an existing temperature-dependent function for maximum per capita growth rate (r_A) and data for the thermal response of algal carrying capacity (K_A) for *Scenedesmus* sp. (Xin et al. 2011). The functions for these parameters (r_A and K_A) were each scaled by a constant factor to give reference values (at 20°C) close to those used by Strauss et al. (2015). This approach preserves the temperature dependence from Xin et al. (2011), while producing more realistic grazer-resource dynamics in our model. The half-saturation constant (h) in the spore yield function was taken from previously published data (Strauss et al. 2015).

Methods: Fitting the Functions. We fit temperature-dependent functions for each trait using Bayesian inference with vaguely informative priors. The functions were fit with replicate-level data (individual hosts for life table experiment and foraging rate assay, beakers for infection assay) from all temperature treatments simultaneously (i.e., propagating all error), implemented with the R2jags package (Plummer 2003; Su and Yajima 2009) in R. We used similar methods to estimate the value of traits at each temperature individually. These point estimates provide graphical insight (fig. 2), but subsequent R_0 calculations and so forth used predicted values from the functions across the temperature-gradient.

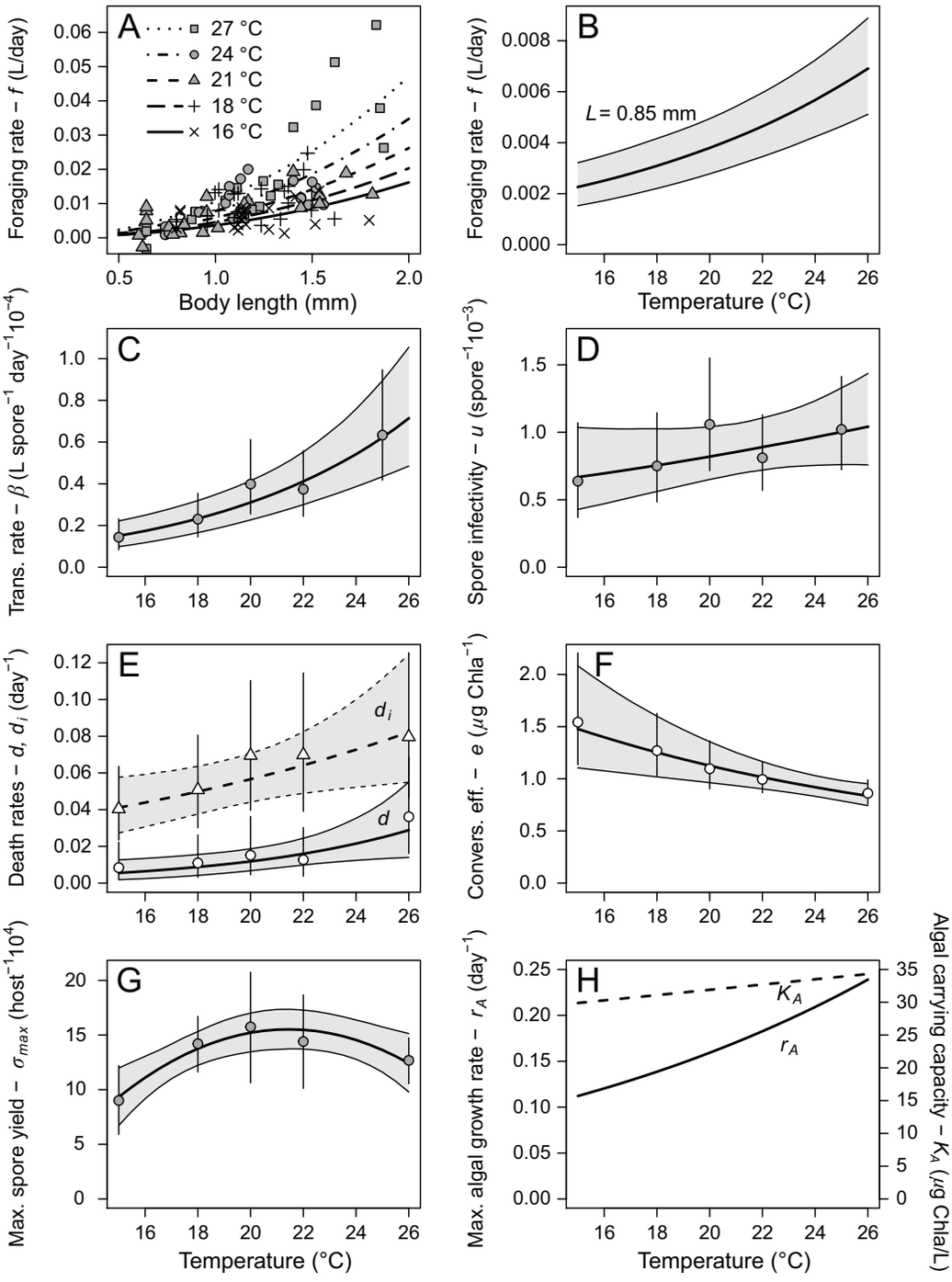

Figure 2: Host, parasite, and resource traits as functions of temperature (also see table 1). *A*, Host foraging rate (f) as a function of body size and temperature. *B*, Host foraging rate (f) for a body length (L) of 0.85 mm (typical population average). *C*, Population transmission rate (β, for $L = 0.85$). *D*, Spore infectivity (u). *E*, Death rates of uninfected (d) and infected hosts (d_i). *F*, Conversion efficiency of births of hosts (e). *G*, Maximal spore yield ($\sigma_{\max}$). *H*, Growth rate of algae (r_A) and algal carrying capacity (k_A). Functions were fit by Bayesian inference. Thick lines are medians of the probability density function; thin lines with gray shading are 95% credible intervals. Points are observed data (*A*) or Bayesian estimates of traits (*C*–*G*) from data at a single temperature treatment (with 95% credible intervals). Resource functions (*H*) are modified from published values (see table 1; Xin et al. 2011).

We used several different thermal functions to map traits to temperature. We used the Arrhenius function to model adult transmission rate (β_{adult}), death rates of susceptible and infected hosts (d and d_i, respectively), and host intrinsic rate of increase (r). The Arrhenius function mechanistically captures the exponentially increasing portion of a thermal reaction norm (Hall et al. 2006; Kooijman 2009). In this approach, the trait value (y) at any temperature (T), $y(T)$, depends on the trait value (y_R) at a reference temperature ($T_R = 20°\text{C}$) and an Arrhenius coefficient (T_A) governing how steeply the trait scales with temperature:

$$y(T) = y_R \cdot e^{T_A(1/T_R - 1/T)}. \tag{2}$$

The foraging rate (f) function uses this Arrhenius function (eq. [2]) but also includes a power function of body length (L), with power coefficient γ and size-specific foraging at 20°C, f_R:

$$f(T, L) = L^{\gamma} \cdot f_R \cdot e^{T_A(1/T_R - 1/T)}. \tag{3}$$

Thus, foraging increases almost exponentially with temperature but also scales with a power of body length. Maximal spore yield ($\sigma_{\max}$) responded unimodally to temperature, T. Thus, we fit a quadratic function of temperature (Angilletta 2006), according to

$$\sigma_{\max}(T) = \alpha_2 \cdot T^2 + \alpha_1 \cdot T + \alpha_0, \tag{4}$$

where the α_2, α_1, and α_0 parameters are fitted constants.

The thermal responses for derived traits were calculated by numerically combining the output of these functions (eq. [2]–[4]) over the temperature gradient. Specifically, we calculated posterior distributions for conversion efficiency (e), spore infectivity (u), and population-level transmission rate (β) by combining the posterior distributions of their component traits (see descriptions above and table 1).

Results. All of the host and parasite traits changed with temperature (fig. 2; table 1). Foraging rate (f) also increased with host body length by approximately length squared (i.e., proportional to host surface area; fig. 2*A*). Foraging rate (f) increased over the entire temperature range. For hosts with body length equal to the natural population average ($L = 0.85$ mm), foraging rate increased by a factor of 3 over this temperature range (fig. 2*B*). Because foraging rate controls host exposure to parasites, it is unsurprising that transmission rate (β) also increased over the entire temperature range. For hosts with body length equal to the natural population average ($L = 0.85$ mm), transmission rate increased by a factor of 4.7 (fig. 2*C*). Accounting for the contribution of exposure to transmission rate, spore infectivity (u) increased weakly over the entire temperature range, by a factor of 1.6 (fig. 2*D*). The death rates of both uninfected hosts (d) and infected hosts (d_i) increased over the entire temperature range by factors of 5.2 and 2.0, respectively (fig. 2*E*). Thus, the death rate of uninfected hosts increased more strongly with temperature, even though the death rate of infected hosts was higher overall. Host birthrate (b) increased over the entire temperature range, by a factor of 1.7 (see fig. A2*B*). However, because birthrate (b) increased less than foraging rate (f), conversion efficiency (e) decreased over the entire temperature range, by a factor of 0.57 (fig. 2*F*). Maximal spore yield initially increased with temperature and then decreased, peaking at 21.5°C, with a spore yield 1.7 times (70%) higher than the minimum at 15°C (fig. 2*G*).

Predicting Disease Spread (R_0)

Methods. We used a common metric of disease spread, R_0, to quantitatively combine the temperature-dependent functions for all of the traits. Here R_0 is an invasion criterion that estimates the parasite population growth rate in a disease-free host population at equilibrium. We calculated R_0 for the model (eq. [1]) using the next-generation matrix approach (Diekmann et al. 2010). The resulting quantity is the ratio of gains (numerator) to losses (denominator) of the parasite:

$$R_0 = \frac{\beta \cdot S_b^* \cdot \sigma_{\max}(A_b^*/A_b^* + h)}{m + f \cdot S_b^*}, \tag{5}$$

where gains stem from infections at transmission rate (β) of susceptible hosts (S_b^*, S at the disease-free boundary equilibrium) and the release of spores. Spore production depends on the maximal yield ($\sigma_{\max}$), the density of algae (A_b^*, A at the disease-free boundary equilibrium), and a half saturation constant (h). Losses come from various background sources (at rate m) and consumption by hosts (at foraging rate f). Equilibrial expressions for algal resource density (A_b^*) and host density (S_b^*) at the disease-free boundary are

$$A_b^* = \frac{d}{e \cdot f}, \tag{6a}$$

$$S_b^* = \frac{r_A}{f}\left(1 - \frac{A_b^*}{K_A}\right), \tag{6b}$$

where A_b^* (eq. [6a]) is the minimal resource requirement of the host; it is the ratio of background per capita death (d) to the slope of birthrate (ef). Host density (eq. [6b]) is then a function of A_b^*, f, and producer traits (maximal per capita growth rate, r_A, and carrying capacity, K_A). (It is the ratio of primary production, per unit algal resource, divided by foraging rate.) For the analyses of R_0, A_b^*, and S_b^*, we used foraging rate (f) calculated for the average body length in a natural population ($L = 0.85$ mm).

We used sensitivity analysis (following Mordecai et al. 2013) to identify which traits in equations (5), (6) most

strongly influenced how R_0 changed with temperature. We also analyzed the two components of transmission rate (β): foraging rate as it contributes to host-spore contact (f_β) and spore infectivity (u). We calculated the partial derivative of R_0 with respect to each trait y ($\partial R_0/\partial y$), scaled per unit of R_0 ($1/R_0$). Multiplying this quantity by the derivative of the trait y with respect to temperature (dy/dT) gives the trait's contribution to the change in R_0. Thus, for a generic trait (y), the contribution of that trait to changes in R_0 is equal to the quantity

$$\frac{1}{R_0}\frac{\partial R_0}{\partial y}\frac{dy}{dT}, \tag{7}$$

which is calculated across the temperature gradient. Sensitivity analyses were conducted using Mathematica 8 (Wolfram-Alpha; see appendix for details).

Results. The two predicted equilibrial densities in R_0 pull against each other. Algal density (A_b^*) at the disease-free boundary equilibrium increases with temperature (T; fig. 3*A*), while host density (S_b^*) decreases with T (fig. 3*B*). Increasing A_b^* should promote disease with higher T (since spore production increases with A_b^*). On the other hand, decreasing S_b^* should reduce disease with higher T (since the positive effect of new infections in the numerator dominates the disease-suppressing effect of susceptible hosts as spore removers in the denominator). Overall, the index of disease spread (R_0) increases over the entire temperature range, although it begins to level off at high temperatures (fig. 3*C*). Therefore, epidemics should become larger in warmer conditions.

The sensitivity analysis reveals which traits are responsible for R_0 increasing with temperature. Transmission rate (β) most strongly drives the increase of R_0 over most temperatures ($T > 16.5$°C), and its effect is essentially constant over the entire range of T (fig. 3*D*). On the other hand, the effect of spore yield (σ_{max}) changes with T and is most important at cold temperatures ($T < 16.5$°C). Low spore production when cold keeps R_0 low (so R_0 is sensitive to any increase in σ_{max} with T); as spore yield increases with warming, it contributes to the rise of R_0. Then, as spore yield decreases from its maximum (at 21.5°C), its contribution to R_0 becomes negative, eventually causing R_0 to begin leveling off. Increasing foraging rate (f, considered here as it appears in eq. [5], i.e., as spore removal only) and decreasing host density (S_b^*) both lower R_0 as T increases (since higher f means fewer spores remain in the environment and decreasing S_b^* means fewer hosts are present to become infected). Increasing algal density raises R_0 as T increases (since more algal resources elevate spore production). However, the magnitude of the impact of these three factors (f, S_b^*, A_b^*) is minimal relative to the other two components (β, σ_{max}), and they essentially cancel each other out. Both mechanistic components of transmission rate (β)—foraging rate as it contributes to host-spore contact (f_β) and spore infectivity (u)—increase R_0 (fig. 3*E*). The former contributes approximately two-thirds of the increase of β, while the latter contributes approximately one-third. For an in-depth analysis of foraging rate (f) and the other components of algal (A_b^*) and host density (S_b^*), see the appendix.

Test of Predictions: Mesocosm Experiment

Methods. We directly tested the prediction that warmer temperatures promote disease spread with a mesocosm experiment at 15.5°, 18.5°, and 23°C. Each replicate tank ($N = 3$ per temperature) was filled with 33 L of water (50% high hardness COMBO [Baer and Goulden 1998] and 50% filtered lake water [A/E filters, 1.0 μm pore size]), inoculated with a nutritious algae (*Scenedesmus acutus*), and lighted to support algal growth. Nutrients were elevated to 20 μg/L phosphorus (as K_2HPO_3) and 300 μg/L nitrogen (as $NaNO_3$) and replaced assuming a 5% loss rate per day. We reared the same host genotype used previously at 23°C and distributed hosts among tanks. After 10 days, we initiated epidemics (with the addition of 6.2 spores/mL). Host densities did not differ significantly between treatments when the spores were added (ANOVA $P = .76$, average 59.6 hosts/L, standard error [SE] = 4.6). Experimental epidemics ran for 56 days after spores were added (3–5 parasite generations, depending on temperature treatment).

We sampled mesocosms to track infection prevalence, host density, and resource density every 3–5 days. To collect samples, we sieved (80 μm) 0.75 L of water to collect hosts (water was returned to the mesocosm). All hosts were diagnosed for infection using a dissecting microscope (×20–×50 magnification). We pooled and homogenized batches of infected hosts from each tank to estimate mean spore load. (The term "spore load" here is used to differentiate spore number measured in live animals at a variety of infection stages vs. "spore yield" in the life table, where animals died due to infection.) We also measured algal density (via chlorophyll *a*, measured using narrow band fluorometry following chilled ethanol extraction [Welschmeyer 1994]).

We tested for the effect of temperature on epidemic size (integrated area under the prevalence time series) using a linear model in R. As in "Field Survey," we log transformed epidemic size, which resulted in an exponential (rather than linear) relationship between temperature and epidemic size. We fit linear mixed effects models predicting spore load and algal density over the whole experiment using similar methods as in "Field Survey." Tank (random) was nested within temperature (fixed, treated as a factor). Sampling day was initially included as a fixed factor but was not significant

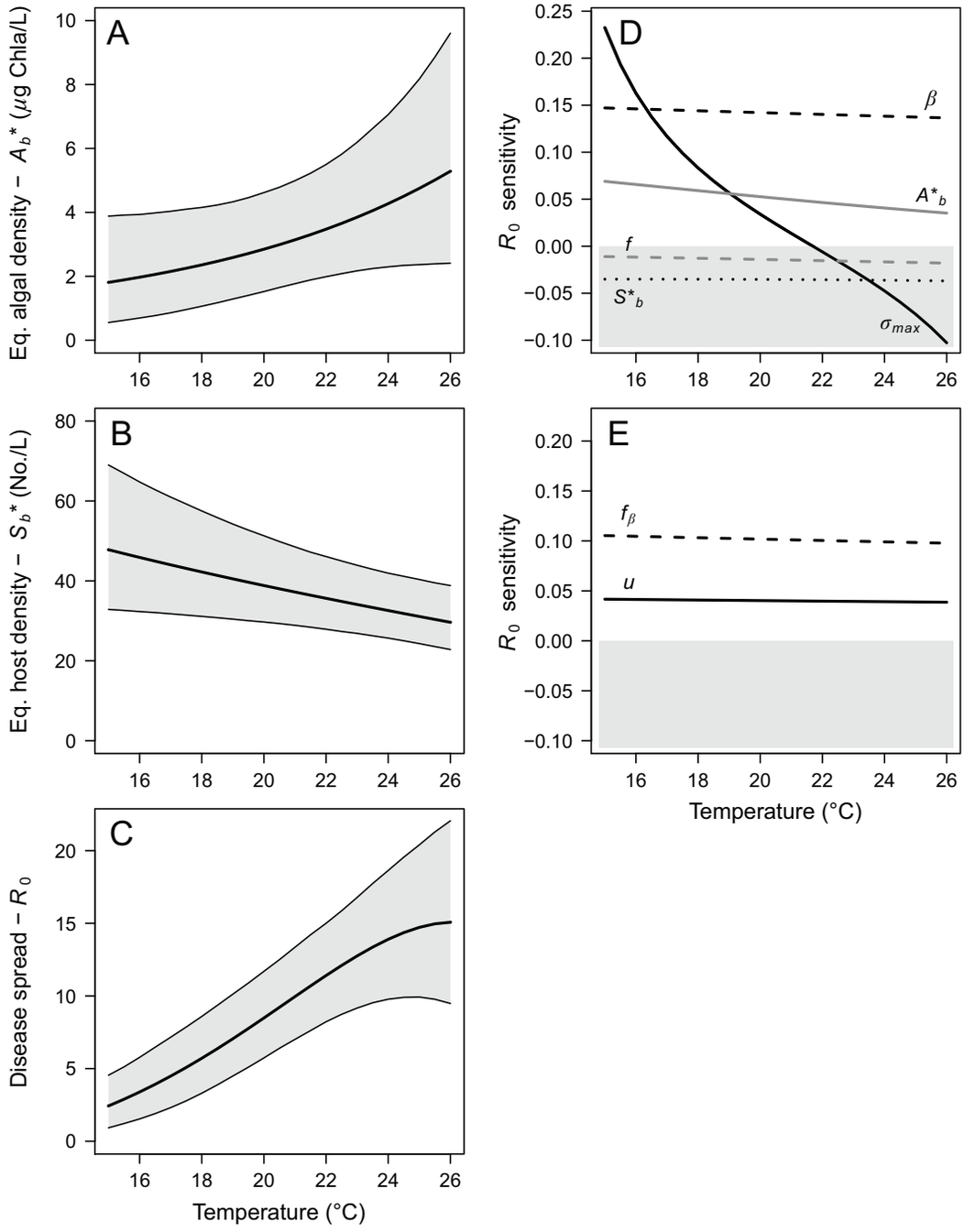

Figure 3: Temperature-dependent functions for density of algae at the disease-free boundary equilibrium, A_b^* (eq. [6a]; *A*), density of hosts at the disease-free boundary equilibrium, S_b^* (eq. [6b]; *B*), and R_0, a measure of disease spread (eq. [5]; *C*). Thick lines are medians of the probability density function. Thin lines with gray shading are 95% credible intervals. *A*–*C* were calculated by combining temperature-dependent functions of host, parasite, and resource traits (see fig. 2). *D*, *E*, The sensitivity of R_0 to its component traits: the sensitivity describes the effect of the thermal response of each trait (y) on the value of R_0, scaled per unit of R_0 (see eq. [7]). A positive value means the trait is causing R_0 to increase (white area), while a negative value means the trait is causing R_0 to decrease (gray shaded area). *D*, The sensitivity of traits as they appear in (eq. [5]): sensitivity to maximal spore yield (σ_{max}: solid black line), transmission rate (β: hashed black line), equilibrium density of algae (A_b^*: solid gray line), foraging rate as it contributes to spore removal (f: hashed gray line), equilibrium density of hosts (S_b^*: dotted gray line). *E*, The sensitivity of R_0 to the two components of transmission rate: foraging rate as it contributes to host-spore contact (f_β) and spore infectivity (u).

for either model ($P = .68$ and $P = .14$, respectively). For spore load, tank was not significant ($P = 1$). For algal density, we included autocorrelation ($\phi = 0.64$). Because of the autocorrelation structure, we could not perform a likelihood ratio test on the tank effect; however, the variance captured by the tank effect was incredibly low (standard deviation $= 2.0 \times 10^{-5}$).

Simulations of Epidemics Using the Parameterized Model. We simulated epidemics for the three temperatures used in the mesocosm experiment (15.5°, 18.5°, and 23°C) using the mathematical model (eq. [1]). Parameter values for host and parasite traits were sampled randomly from the posterior distributions at each temperature. Resource traits used the single values estimated from the temperature-dependent functions. Simulations were run with the deSolve package (Soetaert et al. 2010).

Results. The mesocosm results support the prediction that epidemics should become larger as temperature increases (fig. 4*A*, 4*B*). Epidemic size increased exponentially with temperature (fig. 5*A*; $P < .0001$, adjusted $R^2 = 0.94$). However, while the simulated epidemics make accurate qualitative predictions for the mesocosm, they do not make accurate quantitative predictions for the time-series dynamics (fig. 4*C*). The dynamical model is extremely sensitive to changes in transmission rate (β). As parameterized from the lab assays, it overpredicts the epidemic size and speed of disease spread for the warmest treatment (23°C) and underpredicts these quantities for the coldest treatment (15.5°C). More generally, the model does not capture the successive waves of infections that appear in all of the temperature treatments. Instead, the model predicts a constant increase in infection prevalence until the system reaches an equilibrium. Thus, this model is not a good tool for accurately predicting time series dy-

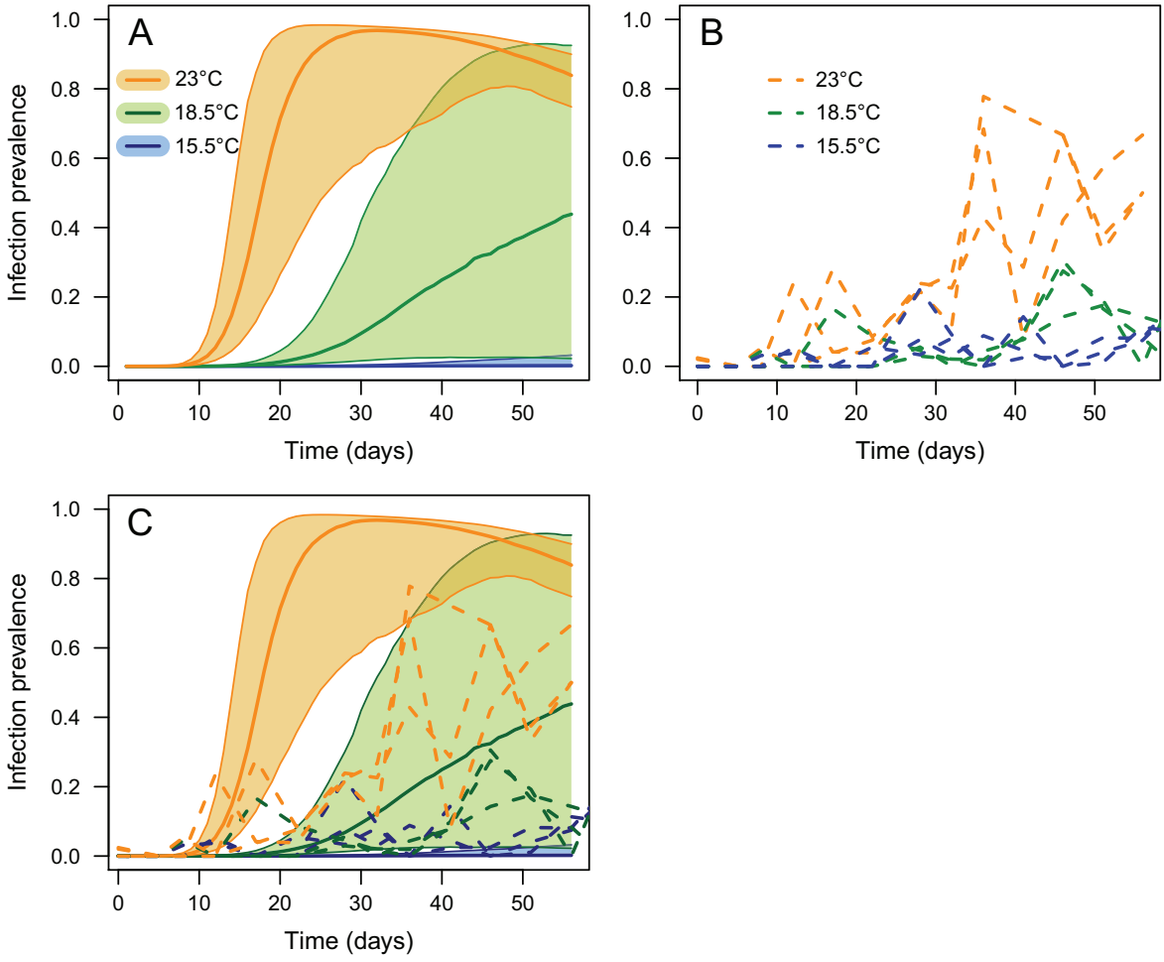

Figure 4: Predictions from model simulations (*A*) and results (*B*) from experimental mesocosms for infection prevalence (i.e., proportion infected) during epidemics. *A*, Model simulations used parameters randomly sampled from the posterior distributions of trait values at each temperature. Thick lines show median values and shaded areas show 67% intervals from 1,000 simulations. *B*, Time series from mesocosm replicates. *C*, Both panels plotted together. In all panels, 15.5°C is blue, 18.5°C is green, and 23°C is orange.

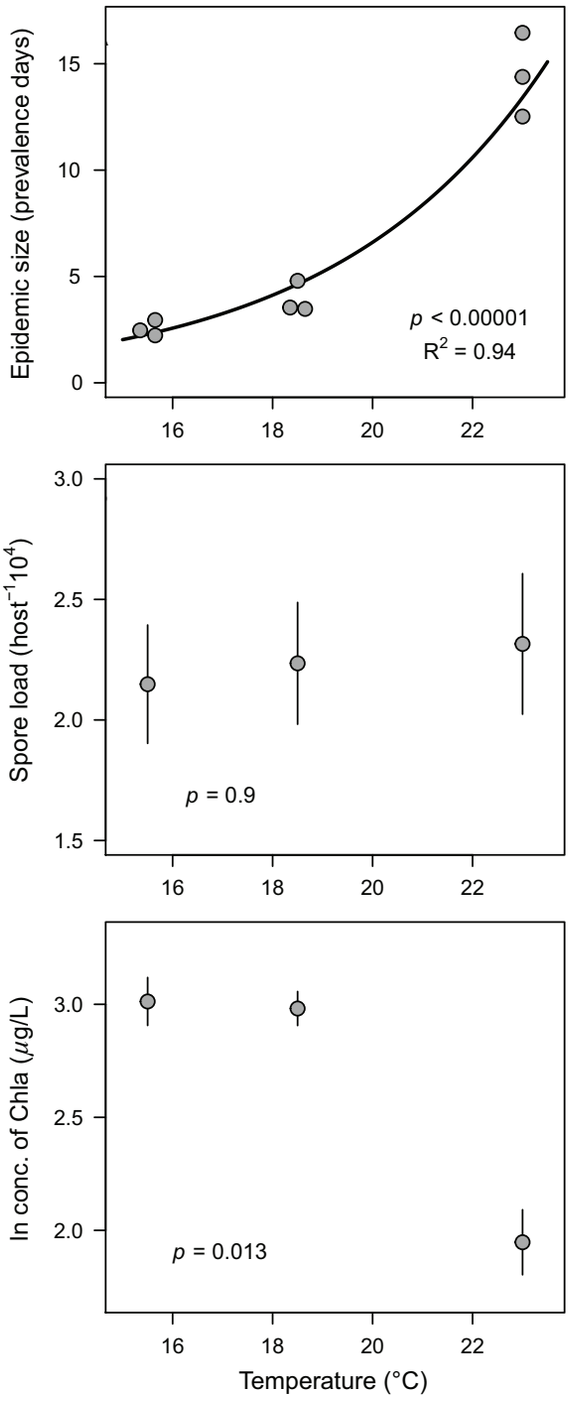

Figure 5: Data from a mesocosm experiment manipulating temperature. *A*, Epidemic size (summed area under the time series curve of infection prevalence) increased with temperature. The curve is a linear model fit to log-transformed epidemic size ($P < .0001$, adjusted $R^2 = 0.94$). Points are jittered for visual clarity. *B*, Spore load (spores per infected host, harvested randomly during sampling) did not vary between temperature treatments (mixed effects model: $P = .9$). *C*, Density of algae (measured as concentration of chlorophyll *a*) was lower at 23°C than at 15.5°C and 18.5°C (mixed effects model: temperature $P = .013$). *B*, *C*, Error bars show standard error through time and across replicate tanks.

namics or values of infection prevalence. Instead, we use it as a guide to make qualitative predictions for how temperature impacts disease spread and epidemic size.

Based on the spore yield (σ_{max}) results from the trait assay, we predicted that spore load would be lower in the 15.5°C treatment than in the two warmer treatments. However, spore load did not vary with temperature (fig. 5*B*; mixed effects model: $P = .90$). Spore production also depends on quantity of algal resources (Civitello et al. 2015). Thus, low algae at higher temperatures might explain the flat thermal response of spore load. There was less algae at 23°C than at the two cooler temperatures (fig. 5*C*; mixed effects model: $P = .013$; see appendix for extended discussion). Low algae could explain flat spore load at 23°C but not why it did not increase at 18.5°C relative to the other temperatures. Nonetheless, based on this flat response, we infer that experimental epidemics grew larger with warming due to increasing transmission rate (β) and remained constrained at low temperatures by low transmission rate.

Thermal Response of Spore Load in Natural Epidemics

Methods. We returned to the lake survey to further evaluate the thermal plasticity of spore load. In the life table experiment, spore yield (spores upon death from infection) responded unimodally to temperature. However, spore load (spore content of randomly selected infected individuals) did not differ in the mesocosm experiment, despite a wide temperature range from 15.5° to 23°C. Thus, we asked, does spore load in nature remain fairly flat (and variable) with temperature? Using spore load data from 2010 (13 lakes) and 2014 (23 lakes), we fit linear mixed effects models predicting spore load on a given sampling date as a function of lake (random), year (fixed), and water temperature (fixed) using similar methods as in "Field Survey." In both models, lake was significant (both models: $P = .0001$), but year was not (weighted temperature: $P = .44$; epilimnetic temperature: $P = .6$). See appendix for details.

Results. The field data show a quadratic relationship between spore load and temperature for weighted temperature (fig. 6*A*; $P = .02$ compared to null model without temperature). However, this thermal effect was small: temperature explained only 3.8% of the variation in spore load (marginal $R^2 = 0.038$). Furthermore, there was no relationship between spore load and epilimnetic temperature (fig. 6*B*; $P = .37$). Additionally, in the relationship with weighted temperature, spore load peaked at 15.4°C, substantially lower than the peak temperature for spore yield in the trait assay (21.5°C). Thus, over a significant temperature range

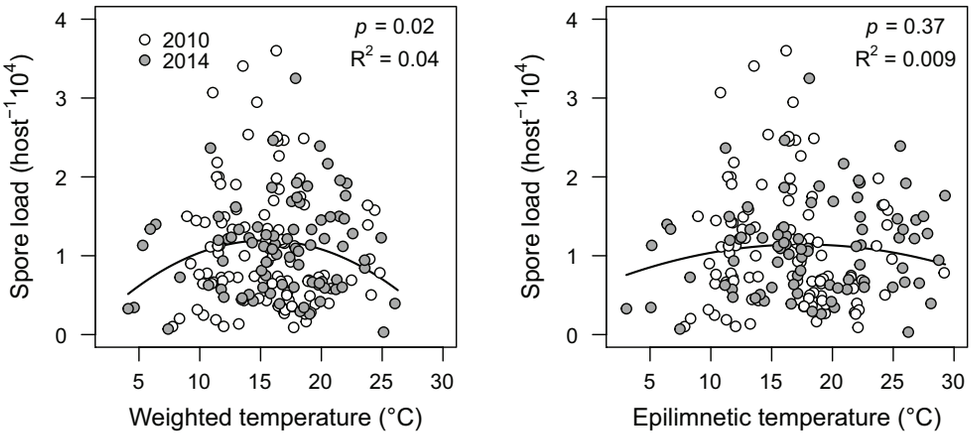

Figure 6: Field data from 2 years show spore load (spores per host, sampled randomly from living infected hosts) as a function of two measures of lake water temperature, weighted temperature (*A*) and epilimnetic temperature (*B*). Infected animals were collected from epidemics in 13 lakes in 2010 and 23 lakes in 2014. Each point is a lake on a single sampling date. The curves are linear mixed effects models predicting spore load from temperature (with both a linear and a quadratic term) and lake as a random effect. *A*, For weighted temperature, $P = .02$ compared to null model without temperature. *B*, For epilimnetic temperature, $P = .37$ compared to null model without temperature.

($15.4°C < T < 21.5°C$), a contradiction arose: spore load decreased slightly in the field but increased to its peak in the trait assay. Overall, given the fairly flat relationship in the field (like in the mesocosm experiment), we conclude that the spore load responds too weakly to temperature in nature to increase epidemic size with temperature (see fig. 1*A*). The thermal response of spore yield might contribute to the waning of natural epidemics at even colder temperatures (<15°C; see fig. 6). Nonetheless, we still conclude that thermal response of transmission rate likely matters more than that of parasite production in nature.

Discussion

To what extent, and through what mechanisms, does temperature drive variation in infectious disease? The answer has important implications for predicting future impacts of climate change on disease. To help answer this question, we investigated the thermal ecology of a freshwater zooplankton-fungus model system. In this system, epidemics start at various times during autumn. Given these staggered starts, seasonal cooling of lakes creates variation in temperature regimes for epidemics. Field data demonstrated that epidemics that started earlier and warmer grew much larger. A mechanistic model parameterized with lab experiments revealed that this temperature-epidemic size pattern could stem from the temperature dependence of transmission rate (β). The thermal response of transmission rate was predominantly governed by exposure (foraging) rate of hosts (f) rather than by spore infectivity (u). We then confirmed that warmer temperatures caused larger epidemics with a population-level experiment in mesocosms. Thus, in warmer environments, increased foraging of hosts increases their exposure to parasites, resulting in more transmission and bigger epidemics.

Warmer temperatures promote disease over the relevant thermal range of our host, in contrast to the few mechanistic models that exist for other systems. More commonly, disease spread or severity peaks at intermediate temperatures. This pattern arises in helminthic parasites of Arctic ungulates (Molnár et al. 2013), schistosomiasis (Mangal et al. 2008), human malaria (Mordecai et al. 2013), and dengue fever (Mordecai et al. 2017). In each of these models, the intermediate peak stems from increased mortality of a key host and/or of the parasite at higher temperatures. For instance, high temperatures elevate mosquito mortality, thereby strongly limiting the spread of human malaria and dengue fever (Mordecai et al. 2013, 2017). The intermediate peak in schistosomiasis is driven by increasing mortality of both the snail host and the free-living parasite stages (Mangal et al. 2008). For the helminths in arctic ungulates, free-living parasite mortality is most important for limiting disease at high temperatures (Molnár et al. 2013). Thus, higher host or parasite mortality under warm conditions is the key trait for many systems where disease spread peaks at intermediate temperatures. In the *Daphnia*-fungus system here, in the relevant temperature range considered, similar mortality factors were not strong.

In contrast, transmission rate (β) drives the warmer-sicker relationship in this plankton case study. Transmission rate dominates disease spread because it directly generates new infections, it increases exponentially with temperature over the relevant thermal range, and it is unconstrained by other

traits. Transmission rate itself depends mechanistically on foraging rate (f; since hosts contact spores while feeding) and spore infectivity (u). Both f and u increase with temperature. Therefore, in warmer environments, hosts contact more fungal spores and are more likely to become infected given exposure. However, foraging rate most strongly drives transmission rate (approximately two-thirds of the thermal response). The thermal response of foraging may generally create a positive relationship between temperature and disease when poikilothermic hosts eat parasites. For example, higher temperatures increase outbreak size by increasing consumption of baculovirus particles on leaves by armyworm caterpillars (Elderd and Reilly 2014). However, transmission rate plateaued at high temperatures in another *Daphnia* disease system with foraging-based exposure (bacteria *Pasteuria ramosa*; Vale et al. 2008). Thus, foraging controlled exposure to parasites may or may not cause transmission rate to increase with temperature. Thermal plasticity of transmission, therefore, warrants further study.

Spore production responded weakly and inconsistently to temperature. Spore yield (σ, spores at host death from infection) peaked at an intermediate temperature in the trait assay. Parasite load is also maximized at intermediate temperatures for nematode parasites in slugs (Wilson et al. 2015), *Ribeiroia* trematodes in their snail intermediate hosts (Paull et al. 2012), and *P. ramosa* bacteria in *Daphnia* (Vale et al. 2008). (But parasite load can also peak at low temperatures: plague bacteria in fleas [Williams et al. 2013], *Providencia* bacteria in fruit flies [Lazzaro et al. 2008], and *Holospora* bacteria in paramecium [Fels and Kaltz 2006]). Based on the R_0 model here, the unimodal response of spore yield should enhance the effect of transmission rate (β) at low temperatures (causing even smaller epidemics) and counter it at high temperatures (flattening the response of epidemic size). However, spore load (spores in randomly sampled infected animals) was flat in the mesocosm experiment and was either flat (for epilimnetic temperature) or peaked at a much lower temperature (for weighted temperature) in natural epidemics (15.4°C vs. 21.5°C). Therefore, other drivers of spore load likely matter more than temperature during epidemics. For instance the quality and quantity of algal resources influence spore production (Hall et al. 2009*a*), and lakes with more algae have higher spore load and larger epidemics (Civitello et al. 2015). Algal resources sometimes increase as lakes cool (Hall et al. 2009*a*), possibly countering the influence of temperature on parasite production and causing spore load to peak later in the epidemic season. However, we did not disentangle interactions of food resources, temperature, spore load, and epidemics here. Regardless, while very cold temperatures (<15°C) might still constrain outbreaks via low parasite production, transmission rate remains the central trait connecting warmer temperatures to larger epidemics.

At higher temperatures in the trait assays, transmission rate increased while parasite production declined with warming. Thus, these traits pulled against each other—and similar tension arises between them along other environmental gradients. For instance, copper contamination and low-quality algal food both increase transmission rate but depress spore production (Hall et al. 2009*a*; Civitello et al. 2012). However, the dominant trait varies. For chronic copper exposure, spore yield dominates, suppressing epidemic size (Civitello et al. 2012). For food quality, the dominant trait shifts along a quality gradient (Hall et al. 2009*a*). For potassium concentration in lake water, spore yield is maximized at intermediate levels while transmission rate is unaffected (Civitello et al. 2013). Over these examples, parasite production seems sensitive to environmental factors that influence within-host resource budgets. With thermal physiology alone, foraging-based transmission rate dominated along temperature gradients. Perhaps this trend will prove general in other systems as well.

Temperature can magnify other biotic and abiotic factors that influence disease spread via changes in epidemic timing. In the plankton case study, start date determines the thermal environment. Therefore, any factor that controls the timing of disease emergence will indirectly affect epidemic size via temperature effects. For instance, epidemics start later in lakes with less dissolved organic carbon since these pigmented compounds shield spores from damaging ultraviolet radiation (Overholt et al. 2012). High densities of a spore-eating, resistant competitor species (diluter *Daphnia pulicaria*) also delay epidemic start dates (Penczykowski et al. 2014*a*). These factors postpone the start of epidemics into colder conditions and, thus, indirectly reduce epidemic size through the thermal mechanisms described here. This pattern could matter greatly because epidemics that start earlier and grow larger also have a stronger negative impact on host densities (Hall et al. 2011). Is this type of interaction between temperature and other ecological factors a general phenomenon? It seems likely a priori, given that seasonal outbreaks are common (Altizer et al. 2006) and diseases are often regulated by multiple, seasonally varying climatic and ecological factors (Rohr et al. 2011; Altizer et al. 2013). However, synthesizing the effects of multiple interacting drivers of disease—particularly in a thermally explicit context—remains a challenge (Rohr et al. 2011; but see Strauss et al. 2016).

Four other aspects of thermal ecology could enhance the trait-based approach here. First, a future perspective must embrace temperature variation. Analyses of mosquito-vectored diseases demonstrate how daily variation of temperature influences traits and disease spread (Paaijmans et al. 2009; Liu-Helmersson et al. 2014). While aquatic habitats are buffered from daily fluctuations relative to terrestrial habitats, the host here often (but not always) verti-

cally migrates. Thus, it can experience wide diurnal variation in temperature (which we averaged out here in our weighted temperature calculation; Hall et al. 2005). Second, upper thermal thresholds could limit epidemics more than suggested by this constant temperature approach. Although these hosts cannot survive constant temperatures above 27°C, in summer they can experience hotter temperatures during night (via migrations to the upper, warmer epilimnion). If the fungus is more thermally sensitive than the host, these summer temperatures could exclude disease (Thomas and Blanford 2003). Third, a focus on fungal physiology could help explain the unimodal response of spore yield. Declining spore yield in warm conditions could potentially result from a lower parasite growth rate within hosts, higher virulence causing hosts to die sooner (thus giving parasites less time to replicate), more effective immune clearance, or a combination thereof. (For a similar discussion of bacterial load in fruit flies, see Lazzaro et al. 2008.) Finally, genetic variation in host and parasite thermal responses could also matter quantitatively, since traits like growth rate and susceptibility could show genotype-by-temperature interactions among host clones (Mitchell et al. 2005; see appendix for host growth rate thermal responses among *Daphnia dentifera* clones). Each of these directions would focus the mechanistic framework on other key aspects of hotter temperatures that may also matter in a warmer world.

Disease ecology needs a better mechanistic framework to link temperature to the spread of epidemics. In this study, we used a planktonic disease system to address some key challenges for this framework. We concluded that epidemic size should increase with temperature because transmission rate increases sensitively with warming. This prediction explained why epidemics that started warmer could grow larger in the field (as confirmed in a population-level mesocosm experiment). Thus, temperature-dependent foraging may be the central trait to examine in many systems with foraging-dependent exposure to parasites. With a mechanistic, thermally explicit framework, disease ecologists can tackle the next questions in the context of climate change. For example, warmer, summerlike conditions will extend deeper into autumn (Ibáñez et al. 2010). Will these changes increase disease? Or will other ecological factors that inhibit epidemics also shift and compensate for warmer temperatures? Better connections between thermal physiology and other aspects of ecology will help to anticipate effects of climate change for disease outbreaks.

Acknowledgments

K. Boatman assisted with 2009 and 2010 field sampling, Z. Brown assisted with 2011 field sampling, and A. Bowling assisted with 2014 field sampling. S. Siscoe, R. Ronk, B. Feaster, and T. Stoelting at the Indiana Department of Natural Resources facilitated the field survey. A. Magnante assisted with the mesocosm experiment. Thanks to J. Kruschke, T. E. X. Miller, and the Enhancing Linkages between Math and Ecology program at Michigan State University for advice and instruction on Bayesian inference. A.T.S. and M.S.S. were supported by the National Science Foundation's (NSF) Graduate Research Fellowship Program. D.J.C. and J.L.H. were supported by Environmental Protection Agency Science to Achieve Results fellowships. This work was supported in part by the NSF Department of Environmental Biology (grants 0841679, 0841817, 1120316, 1120804, 1353749, 1353806, and 1354407).

Statement of authorship: M.S.S., S.R.H., C.E.C., and M.A.D. designed the study. M.S.S., A.T.S., J.L.H., M.Š., and D.J.C. collected data. M.S.S. performed analyses. M.S.S. wrote the first draft of the manuscript, and all authors contributed to revisions.

Literature Cited

Altizer, S., A. Dobson, P. Hosseini, P. Hudson, M. Pascual, and P. Rohani. 2006. Seasonality and the dynamics of infectious diseases. Ecology Letters 9:467–484.

Altizer, S., R. S. Ostfeld, P. T. J. Johnson, S. Kutz, and C. D. Harvell. 2013. Climate change and infectious diseases: from evidence to a predictive framework. Science 341:514–519.

Angilletta, M. J. 2006. Estimating and comparing thermal performance curves. Journal of Thermal Biology 31:541–545.

Baer, K. N., and C. E. Goulden. 1998. Evaluation of a high-hardness COMBO medium and frozen algae for *Daphnia magna*. Ecotoxicology and Environmental Safety 39:201–206.

Bartoń, K. 2009. MuMIn: multi-model inference. R package, version 0.12.2. http://r-forge.r-project.org/projects/mumin/.

Bolker, B. M., M. E. Brooks, C. J. Clark, S. W. Geange, J. R. Poulsen, M. H. H. Stevens, and J. S. S. White. 2009. Generalized linear mixed models: a practical guide for ecology and evolution. Trends in Ecology and Evolution 24:127–135.

Civitello, D. J., P. Forys, A. P. Johnson, and S. R. Hall. 2012. Chronic contamination decreases disease spread: a *Daphnia*-fungus-copper case study. Proceedings of the Royal Society B 279:3146–3153.

Civitello, D. J., R. M. Penczykowski, J. L. Hite, M. A. Duffy, and S. R. Hall. 2013. Potassium stimulates fungal epidemics in *Daphnia* by increasing host and parasite reproduction. Ecology 94:380–388.

Civitello, D. J., R. M. Penczykowski, A. N. Smith, M. S. Shocket, M. A. Duffy, and S. R. Hall. 2015. Resources, key traits and the size of fungal epidemics in *Daphnia* populations. Journal of Animal Ecology 84:1010–1017.

Diekmann, O., J. A. P. Heesterbeek, and M. G. Roberts. 2010. The construction of next-generation matrices for compartmental epidemic models. Journal of the Royal Society Interface 7:873–885.

Ebert, D. 2005. Ecology, epidemiology, and evolution of parasitism in *Daphnia*. National Library of Medicine, Center for Biotechnology Information, Bethesda, MD.

Elderd, B. D., and J. R. Reilly. 2014. Warmer temperatures increase disease transmission and outbreak intensity in a host-pathogen system. Journal of Animal Ecology 83:838–849.

Fels, D., and O. Kaltz. 2006. Temperature-dependent transmission and latency of *Holospora undulata*, a micronucleus-specific parasite of the ciliate *Paramecium caudatum*. Proceedings of the Royal Society B 273:1031–1038.

Hall, S. R., C. R. Becker, M. A. Duffy, and C. E. Cáceres. 2010*a*. Variation in resource acquisition and use among host clones creates key epidemiological trade-offs. American Naturalist 176:557–565.

———. 2011. Epidemic size determines population-level effects of fungal parasites on *Daphnia* hosts. Oecologia 166:833–842.

———. 2012. A power-efficiency trade-off in resource use alters epidemiological relationships. Ecology 93:645–656.

Hall, S. R., M. A. Duffy, A. J. Tessier, and C. E. Cáceres. 2005. Spatial heterogeneity of daphniid parasitism within lakes. Oecologia 143: 635–644.

Hall, S. R., C. J. Knight, C. R. Becker, M. A. Duffy, A. J. Tessier, and C. E. Cáceres. 2009*a*. Quality matters: resource quality for hosts and the timing of epidemics. Ecology Letters 12:118–128.

Hall, S. R., J. L. Simonis, R. M. Nisbet, A. J. Tessier, and C. E. Cáceres. 2009*b*. Resource ecology of virulence in a planktonic host-parasite system: an explanation using dynamic energy budgets. American Naturalist 174:149–162.

Hall, S. R., L. Sivars-Becker, C. Becker, M. A. Duffy, A. J. Tessier, and C. E. Cáceres. 2007. Eating yourself sick: transmission of disease as a function of foraging ecology. Ecology Letters 10:207–218.

Hall, S. R., R. Smyth, C. R. Becker, M. A. Duffy, C. J. Knight, S. MacIntyre, A. J. Tessier, and C. E. Cáceres. 2010*b*. Why are *Daphnia* in some lakes sicker? disease ecology, habitat structure, and the plankton. BioScience 60:363–375.

Hall, S. R., A. J. Tessier, M. A. Duffy, M. Huebner, and C. E. Cáceres. 2006. Warmer does not have to mean sicker: temperature and predators can jointly drive timing of epidemics. Ecology 87:1684–1695.

Harvell, C. D., C. E. Mitchell, J. R. Ward, S. Altizer, A. P. Dobson, R. S. Ostfeld, and M. D. Samuel. 2002. Climate warming and disease risks for terrestrial and marine biota. Science 296:2158–2162.

Hite, J. L., R. M. Penczykowski, M. S. Shocket, A. T. Strauss, P. A. Orlando, M. A. Duffy, C. E. Cáceres, and S. R. Hall. 2016. Parasites destabilize host populations by shifting stage-structured interactions. Ecology 97:439–449.

Ibáñez, I., R. B. Primack, A. J. Miller-Rushing, E. Ellwood, H. Higuchi, S. D. Lee, H. Kobori, and J. A. Silander. 2010. Forecasting phenology under global warming. Philosophical Transactions of the Royal Society B 365:3247–3260.

Kooijman, S. A. L. M. 2009. Dynamic energy budget theory for metabolic organisation. 3rd ed. Cambridge University Press, New York.

Lafferty, K. D. 2009. The ecology of climate change and infectious diseases. Ecology 90:888–900.

Lazzaro, B. P., H. A. Flores, J. G. Lorigan, and C. P. Yourth. 2008. Genotype-by-environment interactions and adaptation to local temperature affect immunity and fecundity in *Drosophila melanogaster*. PLoS Pathogens 4:1–9.

Liu-Helmersson, J., H. Stenlund, A. Wilder-Smith, and J. Rocklöv. 2014. Vectorial capacity of *Aedes aegypti*: effects of temperature and implications for global dengue epidemic potential. PLoS ONE 9.

Mangal, T. D., S. Paterson, and A. Fenton. 2008. Predicting the impact of long-term temperature changes on the epidemiology and control of schistosomiasis: a mechanistic model. PLoS ONE 3: e1438.

Mitchell, S. E., E. S. Rogers, T. J. Little, and A. F. Read. 2005. Host-parasite and genotype-by-environment interactions: temperature modifies potential for selection by a sterilizing pathogen. Evolution 59:70–80.

Molnár, P. K., S. J. Kutz, B. M. Hoar, and A. P. Dobson. 2013. Metabolic approaches to understanding climate change impacts on seasonal host-macroparasite dynamics. Ecology Letters 16:9–21.

Mordecai, E. A., J. M. Cohen, M. V. Evans, P. Gudapati, L. R. Johnson, C. A. Lippi, K. Miazgowicz, et al. 2017. Detecting the impact of temperature on transmission of Zika, dengue, and chikungunya using mechanistic models. PLoS Neglected Tropical Diseases 11:e0005568.

Mordecai, E. A., K. P. Paaijmans, L. R. Johnson, C. Balzer, T. Ben-Horin, E. de Moor, A. McNally, et al. 2013. Optimal temperature for malaria transmission is dramatically lower than previously predicted. Ecology Letters 16:22–30.

Nakagawa, S., and H. Schielzeth. 2013. A general and simple method for obtaining R^2 from generalized linear mixed-effects models. Methods in Ecology and Evolution 4:133–142.

Overholt, E. P., S. R. Hall, C. E. Williamson, C. K. Meikle, M. A. Duffy, and C. E. Cáceres. 2012. Solar radiation decreases parasitism in *Daphnia*. Ecology Letters 15:47–54.

Paaijmans, K. P., A. F. Read, and M. B. Thomas. 2009. Understanding the link between malaria risk and climate. Proceedings of the National Academy of Sciences of the USA 106:13844–13849.

Paull, S. H., B. E. Lafonte, and P. T. J. Johnson. 2012. Temperature-driven shifts in a host-parasite interaction drive nonlinear changes in disease risk. Global Change Biology 18:3558–3567.

Penczykowski, R. M., S. R. Hall, D. J. Civitello, and M. A. Duffy. 2014*a*. Habitat structure and ecological drivers of disease. Limnology and Oceanography 59:340–348.

Pinheiro, J., D. Bates, S. DebRoy, D. Sarkar, and R. C. Team. 2009. nlme: linear and nonlinear mixed effects models. R package, version 3.1-131. https://CRAN.R-project.org/package=nlme.

Pinheiro, J. C., and D. M. Bates. 2000. Mixed-effects models in S and S-PLUS. Springer, New York.

Plummer, M. 2003. JAGS: a program for analysis of Bayesian graphical models using Gibbs sampling. Proceedings of the 3rd International Workshop on Distributed Statistical Computing 1–10, Vienna.

R Core Team. 2016. R: a language and for statistical computing. R Foundation for Statistical Computing, Vienna.

Rodó, X., M. Pascual, F. J. Doblas-Reyes, A. Gershunov, D. A. Stone, F. Giorgi, P. J. Hudson, et al. 2013. Climate change and infectious diseases: can we meet the needs for better prediction? Climatic Change 118:625–640.

Rogers, D. J., and S. E. Randolph. 2006. Climate change and vector-borne diseases. Advances in Parasitology 62:345–381.

Rohr, J. R., A. P. Dobson, P. T. J. Johnson, A. M. Kilpatrick, S. H. Paull, T. R. Raffel, D. Ruiz-Moreno, and M. B. Thomas. 2011. Frontiers in climate change-disease research. Trends in Ecology and Evolution 26:270–277.

Sarnelle, O., and A. E. Wilson. 2008. Type III functional response in *Daphnia*. Ecology 89:1723–1732.

Shocket, M. S., A. T. Strauss, J. L. Hite, M. Šljivar, D. J. Civitello, M. A. Duffy, C. E. Cáceres, and S. Hall. 2018. Data from: Temperature drives epidemics in a zooplankton-fungus disease system: a trait-driven approach points to transmission via host foraging. American Naturalist, Dryad Digital Repository, http://doi.org/10.5061/dryad.3k8m3.

Soetaert, K., T. Petzoldt, and R. W. Setzer. 2010. Solving differential equations in R: package deSolve. Journal of Statistical Software 33: 1–25.

Strauss, A. T., D. J. Civitello, C. E. Cáceres, and S. R. Hall. 2015. Success, failure and ambiguity of the dilution effect among competitors. Ecology Letters 18:916–926.

Strauss, A. T., M. S. Shocket, D. J. Civitello, J. L. Hite, R. M. Penczykowski, M. A. Duffy, C. E. Cáceres, and S. R. Hall. 2016. Habitat, predators, and hosts regulate disease in *Daphnia* through direct and indirect pathways. Ecological Monographs 86:393–411.

Su, Y.-S., and M. Yajima. 2009. R2jags: a package for running JAGS from R. R package, version 0.03-08. https://cran.r-project.org/web/packages/R2jags/index.html.

Tessier, A. J., and P. Woodruff. 2002. Cryptic trophic cascade along a gradient of lake size. Ecology 83:1263–1270.

Thomas, M. B., and S. Blanford. 2003. Thermal biology in insect-parasite interactions. Trends in Ecology and Evolution 18:344–350.

Vale, P. F., M. Stjernman, and T. J. Little. 2008. Temperature-dependent costs of parasitism and maintenance of polymorphism under genotype-by-environment interactions. Journal of Evolutionary Biology 21:1418–1427.

Welschmeyer, N. A. 1994. Fluorometric analysis of chlorophyll *a* in the presence of chlorophyll *b* and pheopigments. Limnology and Oceanography 39:1985–1992.

Williams, S. K., A. M. Schotthoefer, J. A. Montenieri, J. L. Holmes, S. M. Vetter, K. L. Gage, and S. W. Bearden. 2013. Effects of low-temperature flea maintenance on the transmission of *Yersinia pestis* by *Oropsylla montana*. Vector Borne and Zoonotic Diseases 13:468–478.

Wilson, M. J., A. J. Digweed, J. Brown, E. S. Ivanonva, and S. H. Hapca. 2015. Invasive slug pests and their parasites—temperature responses and potential implications of climate change. Biology and Fertility of Soils 51:739–748.

Xin, L., H. Hong-ying, and Z. Yu-ping. 2011. Growth and lipid accumulation properties of a freshwater microalga *Scenedesmus* sp. under different cultivation temperature. Bioresource Technology 102:3098–3102.

Zuur, A. F., E. N. Ieno, N. Walker, A. A. Saveliev, and G. M. Smith. 2009. Mixed effects models and extensions in ecology with R. Statistics for Biology and Health. Springer, New York.

References Cited Only in the Online Appendix

Bertram, C. R., M. Pinkowski, S. R. Hall, M. A. Duffy, and C. E. Cáceres. 2013. Trait-mediated indirect effects, predators, and disease: test of a size-based model. Oecologia 173:1023–1032.

Lampert, W., and I. Trubetskova. 1996. Juvenile growth rate as a measure of fitness in *Daphnia*. Functional Ecology 10:631–635.

Penczykowski, R. M., B. C. P. Lemanski, R. D. Sieg, S. R. Hall, J. Housley Ochs, J. Kubanek, and M. A. Duffy. 2014*b*. Poor resource quality lowers transmission potential by changing foraging behaviour. Functional Ecology 28:1245–1255.

Plummer, M. 2013. JAGS, version 3.4.0. User manual. https://sourceforge.net/projects/mcmc-jags/files/Manuals/3.x.

Tessier, A. J., and J. Welser. 1991. Cladoceran assemblages, seasonal succession and the importance of a hypolimnetic refuge. Freshwater Biology 25:85–93.

Associate Editor: Greg Dwyer
Editor: Yannis Michalakis

Daphnia dentifera zooplankton hosts that are infected (*left*) and uninfected (*right*) with fungal parasite *Metschnikowia bicuspidata*. Photo credit: Meghan A. Duffy.